MIXED MODE CRACK-TIP FIELDS IN MONOLITHIC CERAMICS

M. Ortiz and A. E. Giannakopoulos

Division of Engineering, Box D, Brown University, Providence, RI 02912, U.S.A.

Abstract—Asymptotic and full field finite element solutions are given for a semi-infinite planar crack in a monolithic ceramic subjected to remote mixed mode loading. The material is assumed to undergo damage in the form of elastic degradation as a result of stable microcracking. Microcracks are assumed to be preferentially oriented normal to the direction of maximum tension. An outcome of the analysis is that microcracks shield the crack tip less effectively under mode II than under mode I conditions. Other issues addressed concern the relation between the mixities of the applied loads and the near-tip fields, the path-independence of the J integral, the validity of deformation theories of damage under proportional loading, and the conditions for dominance of the singular near-tip fields.

1. INTRODUCTION

A growing body of research is presently concerned with the development of a fracture mechanics of brittle solids such as ceramics. These are materials which, while not undergoing plastic deformations of any significance at low temperatures, can nevertheless behave quite inelastically as a result of the nucleation, growth and coalescence of microcracks. In certain classes of ceramics, extensive intergranular microcracking has indeed been observed in the immediate vicinity of macrocrack tips (Hoagland et al., 1973; Claussen, 1976; Wu et al., 1978).

Despite recent progress in the area, a full understanding of the interplay between microcracking and fracture is yet to emerge. For instance, there is an apparent discrepancy between the measured surface energy of grain boundary facets and the overall toughness of the polycrystalline material. A plausible conjecture which has recently been the subject of intense investigation is that near-tip microcracking accounts for such a discrepancy. The supposition is that, by rendering the material more compliant, microcracks in effect shield the crack tip from the action of the remotely applied loads (Evans, 1984). Thus, interest in the shielding mechanism stems from its potential for enhancing the fracture toughness of ceramics. In reality, the presence of microcracks ahead of the crack tip degrades the intrinsic resistance to fracture of the material, an effect which partially or totally offsets the toughness gains derived from shielding (Ortiz, 1988). It thus appears that the toughness of ceramics may be the result of a combination of toughening mechanisms operating in conjunction with shielding, such as crack deflection (Faber and Evans, 1983a, b) and bridging (Swanson et al., 1987).

Whatever the mechanisms involved, the singular fields which develop in the presence of damage set the outer boundary conditions for the actual processes of crack growth. In this sense, there remains a critical need to understand and characterize such singular fields. Some of the studies completed to date have been based on approximate solutions to many-crack problems (Gong and Horii, 1987; Hoagland and Embury, 1980; Kachanov, 1986). Others have employed models of distributed damage (Evans and Fu, 1985; Charalambides, 1986; Charalambides and McMeeking, 1987; Hutchinson, 1987; Ortiz, 1987; Rodin, 1987). In the latter category, Charalambides (1986) and Charalambides and McMeeking (1987) considered the case of isotropic damage and Ortiz (1987) the case of damage normal to the maximum tensile direction. Hutchinson (1987) based his analysis on dilute microcracking approximations.

All of the above studies, however, have been solely concerned with the case of mode I loading. In this paper, we proceed to investigate the mixed mode case. Asymptotic and full

field finite element solutions are given for the standard problem of a semi-infinite planar crack undergoing plane strain deformations. The material is assumed to undergo damage in the form of elastic degradation as a result of stable microcracking. Microcracks are assumed to be preferentially oriented normal to the direction of maximum tension.

Some of the issues addressed concern the relation between the mixities and stress intensity factors of the remote and near-tip fields, the path independence of the J integral, the validity of deformation theories of damage under proportional loading, and the conditions for dominance of the singular near-tip fields. A rather remarkable result is that the mixities of the remote and near-tip stress fields ostensibly coincide. For the proportional loading conditions investigated here, the computed stress paths are observed to remain nearly proportional. Under these conditions, the constitutive response becomes indistinguishable from that of a nonlinear elastic solid and the J integral applies with its usual path-independence properties. This, in conjunction with the observed conservation of mixities, provides a means for computing the near-tip stress intensity factors directly from the asymptotic solutions.

An outcome of this analysis is that microcracks shield the crack tip less effectively under mode II than under mode I conditions, an observation which is in keeping with the available observational evidence (Shetty *et al.*, 1981; Morrone and Suresh, 1988). This effect is rooted in the fact that the mixed mode asymptotic fields, derived in Section 3, exhibit an elastic wedge where the material is free of damage. This leaves the crack tip partially unshielded from the remote loads.

Finally, we show in Section 4 that the asymptotic fields computed here possess regions of dominance comparable to those found in plastic solids under small scale yielding conditions. Thus it is checked that, under suitable conditions which are enumerated in Section 4, the process zone where the actual separation processes resulting in the advance of the crack take place is indeed deep inside the region of dominance of the asymptotic fields. In particular, crack growth may be expected to be driven by the near-tip stress intensity factors computed in Section 4.

2. DAMAGE MODEL

Stable microcracking in ceramic materials has the beneficial effect of partially relieving the stress concentrations that arise at the tip of a crack, in effect shielding it from the action of remote loads. Extensive microcracking of this type has been observed in certain classes of ceramics (Hoagland *et al.*, 1973; Claussen, 1976; Wu *et al.*, 1978). Microcracks develop mainly at grain boundary facets as a result of residual stresses generated during cooling and of applied tensile stresses (Fu, 1983). Once the microcracks are formed they tend to remain confined to their facets with their tips pinned stably at grain junctures. As the number of microcrack nucleation sites is exhausted a saturation stage ensues during which the material sustains no further damage; see Fig. 1a.

The process of microfracture has the additional effect of relieving grain-to-grain residual stresses which arise during cooling from the fabrication temperature. The magnitude and statistical properties of these residual stresses have been computed analytically by Ortiz and Molinari (1988). At the macroscopic level, the stress relaxation process manifests itself as the development of permanent strains. Thus, upon removal of the loads, the strains do not reduce to zero but rather attain a residual value; see Fig. 1a. Hutchinson (1987) has pointed out the analogy between these irreversible strains and those arising as a result of displacive phase transitions.

Transformation strains have been shown to exert a significant toughening effect on growing cracks; by Budiansky *et al.* (1983) for transforming second-phase particles, and by Charalambides (1986) for microcracking. By contrast, a result of Budiansky *et al.* (1983) asserts that volumetric transformation strains have no effect on the near-tip stress intensity factors of stationary cracks. In addition, transformation strains remain bounded at all levels of stress, and thus contribute negligibly to the near-tip singular strain fields. Consequently, for the purpose at hand, i.e. for the computation of asymptotic fields in stationary cracks, transformation strains may be altogether neglected.
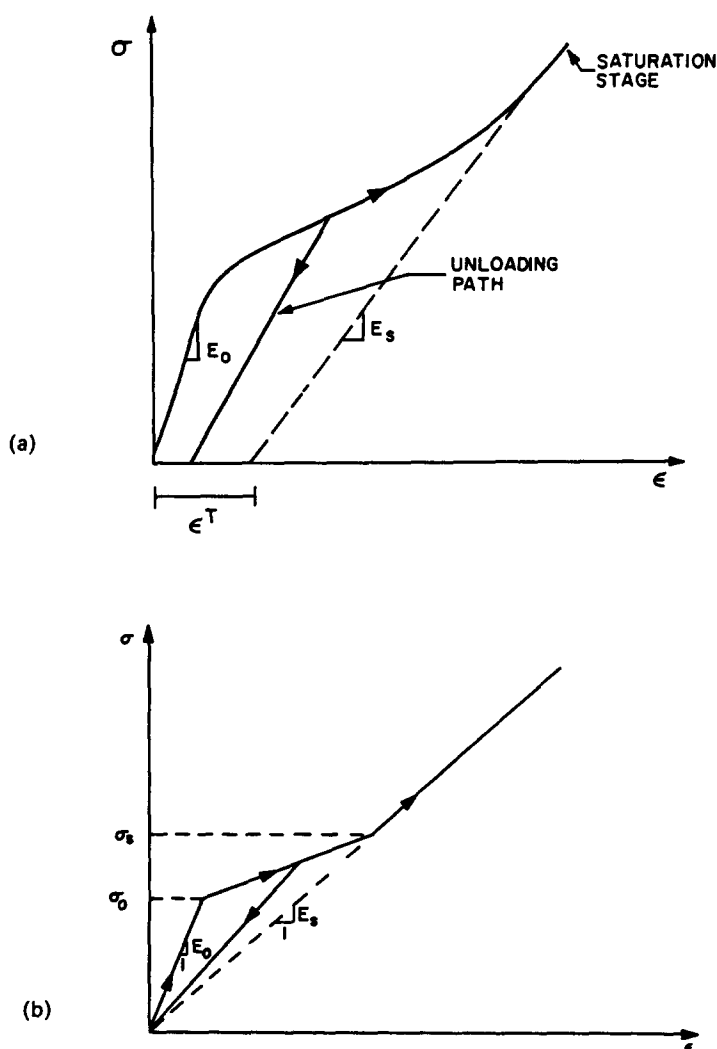
Fig. 1. (a) Stress–strain behavior of monolithic ceramic. (b) Trilinear idealization.

Throughout the present work, it is presumed that the deformation processes of interest involve the cooperative response of large numbers of distributed microcracks. The solid is thus idealized as a homogenized continuum undergoing distributed damage. The particular damage model adopted here conforms to the general framework formulated by Ortiz (1985).

The stresses σ_{ij} and strains ε_{ij} in the solid are assumed to be linearly related according to

$$\varepsilon_{ij} = C_{ijkl}\sigma_{kl} \tag{1}$$

where the elasticity tensor C_{ijkl} is regarded as an internal variable characterizing the current state of microcracking. In this work, attention is confined to the monotonic loading processes in which microcrack closure plays no significant role. A general treatment of microcrack closure as a unilateral constraint has been formulated by Ortiz (1985).

Of primary interest to the applications sought here is the development of damage in *tension*. A wealth of observational evidence exists on microcrack formation in ceramics at elevated temperatures (see Suresh and Brockenbrough, 1989, for a recent review). Under these conditions, microcracks appear to be mainly intergranular and to form preferentially normal to the tensile axis. Similar observations have been made by Hayhurst (1972) and Hayhurst and Leckie (1973) for creep rupture of metals under multiaxial states of stress.

Hayhurst (1972) conducted biaxial tension creep rupture tests on an aluminum alloy and observed that in all cases grain boundary cracks had grown on planes which were at an angle of 90° to the direction of maximum tension. By way of contrast, similar data for ceramics at low temperatures do not seem to be as yet available in the literature. Microcrack observations in rocks are mainly confined to compressive states of stress (see, e.g., the review of Kranz, 1983). It seems reasonable to assume, however, that, as in the high temperature range, microcracks nucleated at low temperatures in multiaxial tension will also tend to be preferentially aligned normal to the maximum principal stress. A damage rule consistent with this assumption is

$$\dot{C}_{ijkl} = \dot{\mu} n_i n_j n_k n_l \qquad (2)$$

where the unit vector n points in the direction of maximum tension and μ may be interpreted as a scalar measure of cumulative damage. For instance, in uniaxial tension μ reduces to $1/E - 1/E_0$, where E is the current secant modulus and E_0 is the initial Young's modulus.

Damage rule (2) has been shown by Ortiz and Giannakopoulos (1988) to maximize the extent of crack-tip shielding. More precisely, of all possible arrangements of a given microcrack density, maximum shielding is obtained when all microcracks develop normal to the direction of maximum tension, as required by (2).

The definition of the model is completed by postulating a suitable equation of evolution for μ. To this end, we start by assuming that incremental damage is possible only if the damage criterion

$$\sigma_1 = \sigma_c \qquad (3)$$

is satisfied. Here, σ_1 is the maximum principal stress. The critical tensile stress σ_c is a function of the state of damage itself, e.g., through the cumulative damage parameter μ.

The dependence of σ_c on μ may be determined simply from the uniaxial tension test (Ortiz, 1988). In this work, we have assumed the trilinear law depicted in Fig. 1b. Thus, following a linear elastic stage characterized by some initial moduli, E_0 and v_0, a linear transition ensures as the elastic limit σ_0 is exceeded. This transitional regime continues up to the saturation stress σ_s, at which the material is assumed to attain a saturated modulus E_s. A stress–strain dependence of this nature has been generally adopted in the majority of the studies on microcrack shielding to date.

Of particular interest to subsequent developments is the behavior of the material under proportional and monotonic stressing. Under these conditions, it may be shown (Ortiz, 1987) that the constitutive response becomes indistinguishable from that of a nonlinear elastic material and may thus be formulated as a deformation theory of damage. In the saturation range, the stress–strain law takes the particularly simple form

$$\varepsilon_{ij} = C^0_{ijkl}\sigma_{kl} + \lambda_s \sigma_1 n_i n_j \qquad (4)$$

where C^0_{ijkl} are the initial elastic moduli and

$$\lambda_s = 1/E_s - 1/E_0. \qquad (5)$$

As will become apparent in the asymptotic analysis that follows, a key feature of stress–strain law (4) is that it derives from a complementary energy potential which is homogeneous of degree two (Ortiz, 1987).

3. ASYMPTOTIC ANALYSIS

Next, we endeavor to characterize the mixed mode crack-tip behavior of solids obeying the constitutive laws formulated in the preceding section. To this end, we consider a body containing a semi-infinite crack on the negative x_1-axis undergoing plane strain
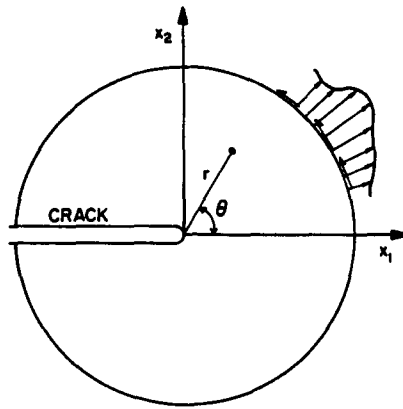
Fig. 2. Definition of boundary value problem.

deformations under the action of a remote mixed mode K-field; see Fig. 2. The boundary conditions appropriate to this problem may be posed as

$$\sigma_{12} = \sigma_{22} = 0, \quad x_1 < 0, \quad x_2 = 0$$

$$\begin{Bmatrix} \sigma_{rr} \\ \sigma_{r\theta} \end{Bmatrix} \to \frac{K_I^{\infty}}{\sqrt{2\pi r}} \begin{Bmatrix} \tilde{\sigma}_{rr}^I \\ \tilde{\sigma}_{r\theta}^I \end{Bmatrix} + \frac{K_{II}^{\infty}}{\sqrt{2\pi r}} \begin{Bmatrix} \tilde{\sigma}_{rr}^{II} \\ \tilde{\sigma}_{r\theta}^{II} \end{Bmatrix}, \quad \text{as } r \to \infty \tag{6}$$

where K_I^{∞} and K_{II}^{∞} are the remotely applied mode I and II stress intensity factors, respectively, and $\tilde{\sigma}_{ij}^I(\theta)$ and $\tilde{\sigma}_{ij}^{II}(\theta)$ the corresponding linear elastic angular fields (see, e.g. Rice, 1968). Here and subsequently, (r, θ) refer to a system of polar coordinates centered at the crack tip with θ measured from the plane of the crack.

A measure of the relative weights of modes I and II in the solution is provided by the mixity ratio

$$M^d = \frac{2}{\pi} \tan^{-1} \left| \frac{K_I^{\text{tip}}}{K_{II}^{\text{tip}}} \right|. \tag{7}$$

With this definition, M^d varies from 0 for mode II to 1 for mode I. A similar measure

$$M^e = \frac{2}{\pi} \tan^{-1} \left| \frac{K_I^{\infty}}{K_{II}^{\infty}} \right| \tag{8}$$

characterizes the modal composition of the applied stress fields.

Let the remote loads be increased proportionally and monotonically. Then, for the class of materials considered here, the resulting near-tip fields possess a tripartite structure; see Fig. 3. In the innermost region, the maximum tensile stress exceeds the saturation stress and the material is saturated. In the outermost region, the stresses lie below the damage threshold and the material is intact. Between these two zones, there lies a transition region where the material is partially damaged.

If the remote loads are increased proportionally, it may be reasonably expected that all material points about the crack tip undergo near-proportional stressing, a presumption which is verified below by way of numerical testing. For proportional stressing, the model outlined in Section 2 reduces to a deformation theory of damage (Ortiz, 1987, 1988). A key feature of the corresponding complementary energy potential is that it is homogeneous of degree two in the saturation stage. Under these conditions, a classical argument of Rice (1968) shows that the asymptotic stress and strain fields must be square-root singular.
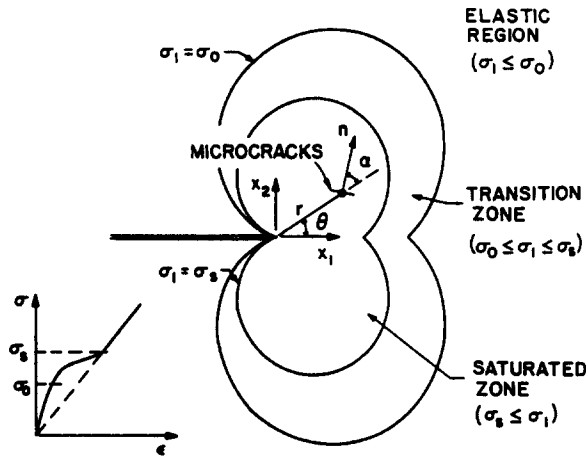
Fig. 3. Elastic, saturated and transition zones in the small scale damage problem for a stationary crack.

Hence, it is possible to introduce a pair of crack-tip stress intensity factors in the usual manner,

$$K_I^{tip} = \lim_{r \to 0} \sqrt{2\pi r} \sigma_{\theta\theta}(r, 0)$$

$$K_{II}^{tip} = \lim_{r \to 0} \sqrt{2\pi r} \sigma_{r\theta}(r, 0). \qquad (9)$$

The net effect of microcracking is to reduce the magnitudes of $(K_I^{tip}, K_{II}^{tip})$ with respect to those of $(K_I^\infty, K_{II}^\infty)$, thus in effect shielding the crack tip from the remotely applied loads. If the near-tip fields dominate over a distance much larger than the size of the process zone wherein the actual separation processes take place, then the criteria for crack growth should be expressible in terms of $(K_I^{tip}, K_{II}^{tip})$, which thus become a central object of the analysis. The issue of dominance is addressed in Section 4.

For the class of materials under consideration, the mode I near-tip fields have been determined analytically by Ortiz (1987). Remarkably, in this case one finds that the stress field exhibits angular variations which are identical to those of the linear elastic solution. Moreover, the amplitude of the singular fields can be computed in closed form by recourse to the J integral of Rice.

The mixed mode and pure mode II cases, by contrast, appear to have heretofore defied analytical characterization. Here we seek to make progress by numerical means. Two different methods of solution are employed. Full field solutions are obtained by means of the finite element method, as discussed in the next section. In asymptotic studies, however, it proves advantageous to exploit the separability of the solution to reduce the problem to a single odinary differential equation for the angular fields. We solve this ODE by means of the finite element method outlined in the Appendix.

Figure 4 shows the angular distributions of the near-tip singular stress fields for various mixities. The results correspond to a choice of material parameters $E_s/E_0 = 0.6$ and $v_0 = 0.25$. All stress components are seen to be everywhere continuous. The symmetry of the mode I fields, Fig. 4a, is lost as soon as a mode II component is introduced in the solution, Figs 4b–4e. By and large, the stress fields obtained in the presence of damage are quite similar, although not identical, to the corresponding elastic fields of the same mixity.

A noteworthy feature of the computed stress fields is the presence of an elastic wedge, i.e. of a sector $(\pi - \theta^e) \leqslant \theta \leqslant \pi$ in which $\bar{\sigma}_1 \leqslant 0$. For mode II, the angle θ^e is plotted in Fig. 5 as a function of the extent of damage. As may be seen, θ^e decreases steadily from a limiting value of roughly $110°$ corresponding to the linear elastic case.

It is interesting to note that the presence of a sector devoid of damage leaves the crack tip partially unscreened. Under these conditions, the net amount of shielding experienced

by the crack tip may be expected to decrease with the extent of mode II in the solution. Figure 6 compares the shielding ratios obtained for modes I and II as a function of the extent of damage. The relation between the remote and near-tip stress intensity factors follows from the assumed path independence of the J integral of Rice. The presumption of path independence is, as noted above, contingent upon the near-proportionality of the stress trajectories at all material points. That this is indeed so is confirmed below with the aid of full field finite element solutions. As expected, the shielding ratio for mode II is consistently lower than that for mode I; see Fig. 6. This observation is in keeping with the experimental data available to date (Shetty *et al.*, 1981; Morrone and Suresh, 1988).
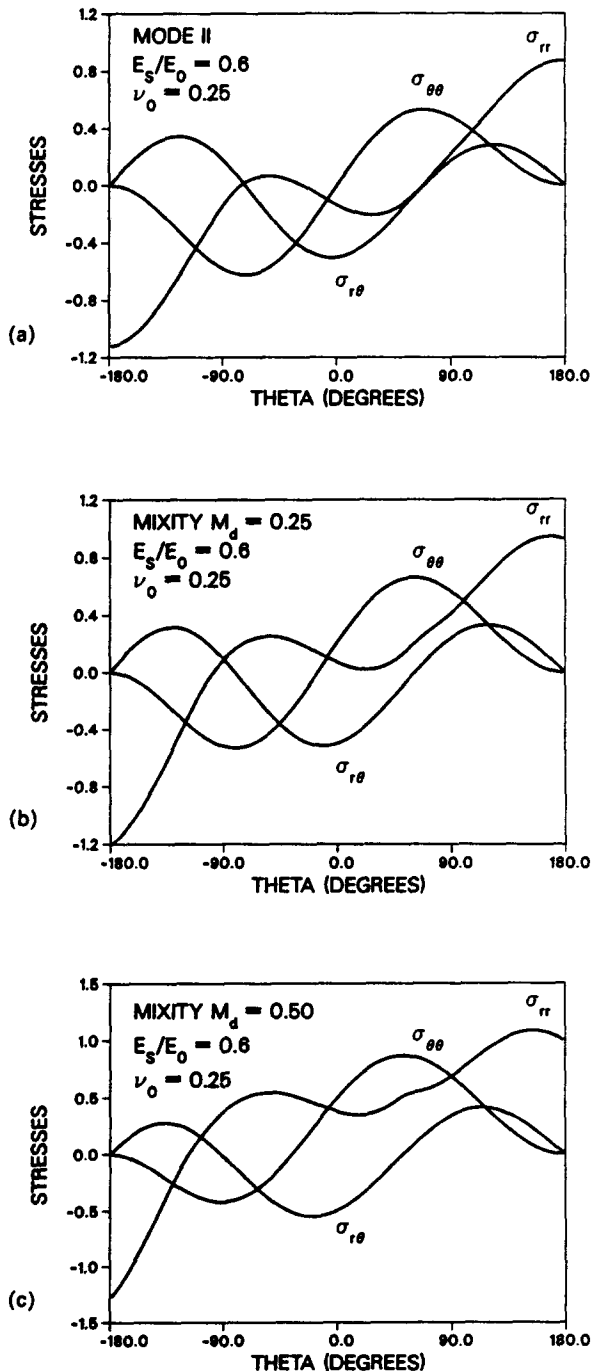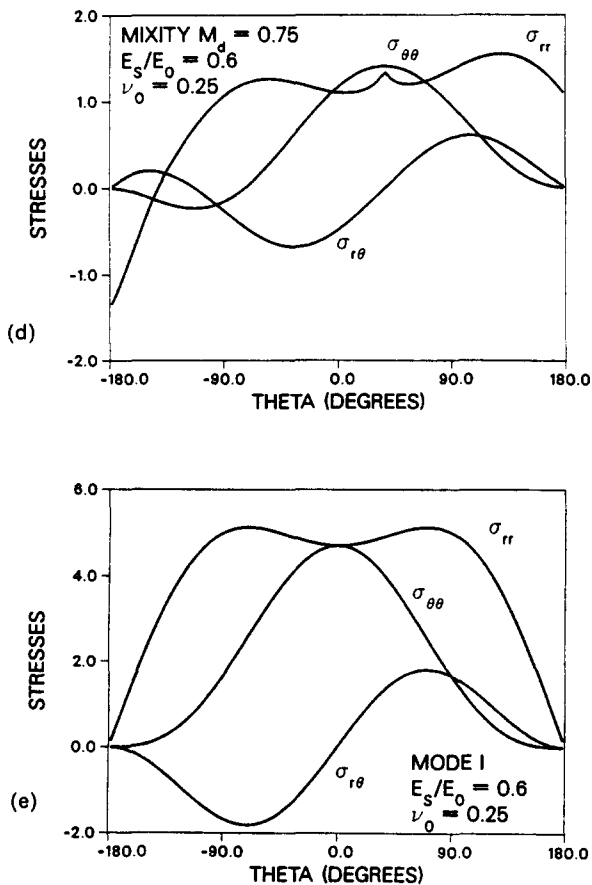

Fig. 4. Near-tip stress fields.

(d)

(e)

Fig. 4—Continued.

As in the mode I case (Ortiz, 1987), the asymptotic strain fields possess a richer structure than the corresponding stress fields. A salient feature of the strains is the presence of discontinuities or jumps. It follows from Maxwell's compatibility conditions (see, e.g., Gurtin, 1984) that the only admissible jumps are $[\![\varepsilon_{\theta\theta}]\!]$ and $[\![\varepsilon_{r\theta}]\!]$. Noting that the stresses are continuous, one finds from constitutive relations (4) that

$$[\![\varepsilon_{\theta\theta}]\!] = \lambda_s \sigma_1 [\![n_\theta n_\theta]\!]$$
$$[\![\varepsilon_{r\theta}]\!] = \lambda_s \sigma_1 [\![n_r n_\theta]\!]. \tag{10}$$
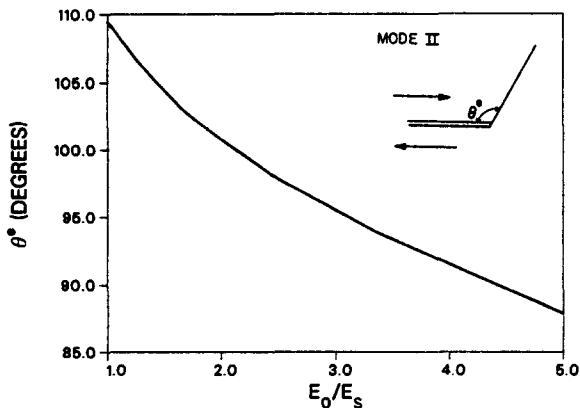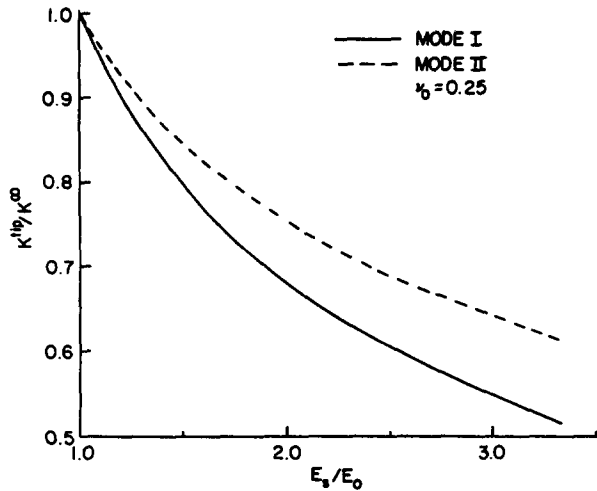

Fig. 5. Amplitude of the elastic sector.

Fig. 6. Shielding ratios for modes I and II.

Let α denote the angle subtended by the direction of maximum tension $\mathbf{n}$ and the radial direction. Thus,

$$\alpha = \tfrac{1}{2}\tan^{-1}\frac{\sigma_{r\theta}}{\sigma_{rr}-\sigma_{\theta\theta}} \tag{11}$$

and $(n_r, n_\theta) = (\cos\alpha, \sin\alpha)$.

By virtue of (11), it follows that strain jumps are possible only if α itself is discontinuous. By inspection of (11) it becomes apparent that α jumps from $-\pi/4$ to $\pi/4$ as $\sigma_{rr}-\sigma_{\theta\theta}$ goes through zero. Moreover, these are the only possible discontinuities of α when the stresses are continuous.

Let $\alpha^{\pm} = \pm\pi/4$. Then, it follows from (10) that

$$\varepsilon_{\theta\theta}^{\pm} = \lambda_s\sigma_1/2$$
$$\varepsilon_{r\theta}^{\pm} = \pm\lambda_s\sigma_1/2. \tag{12}$$

In particular,

$$[\![\varepsilon_{\theta\theta}]\!] = 0$$
$$[\![\varepsilon_{r\theta}]\!] = \lambda_s\sigma_1. \tag{13}$$

All strain jumps in the computed solutions are indeed found to conform to these conditions, i.e. only jumps in $\varepsilon_{r\theta}$ are observed, the jumps occur at points where $\sigma_{rr} = \sigma_{\theta\theta}$, and the amplitudes of the jumps obey (13). From a physical standpoint, the angle α may be viewed as defining the preferred orientation of the microcracks relative to the radial direction. Thus, a jump in α may be interpreted as an indication that two families of microcracks coexist at the point of discontinuity.

4. FULL FIELD FINITE ELEMENT SOLUTIONS

In this section, we present finite element solutions to the problem of a semi-infinite crack under the action of a remote mixed mode K-field. Full field solutions furnish valuable information on features of the singular fields which are not revealed by an asymptotic analysis, such as the zone of dominance of the asymptotic solution and the precise nature of the transition fields. We also seek to verify assumptions that were made as part of the asymptotic treatment of the problem, such as the proportionality of stress paths at all material points in the solid.
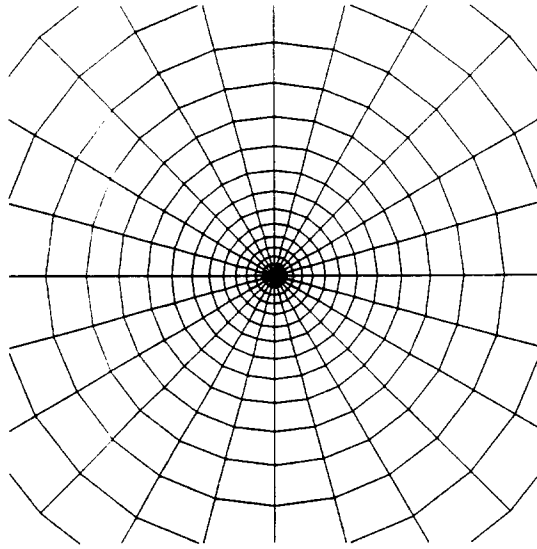
Fig. 7. Finite element mesh employed in full field analysis.

Throughout the calculations, the domain of the analysis was discretized into a fan-like finite element mesh with increasing resolution towards the tip; see Fig. 7. The elements employed were nine-noded isoparametric quadrilaterals. The mesh resolved the domain $-\pi \leqslant \theta \leqslant \pi$ into 48 equal sectors. In mode I, the symmetries inherent to the problem permit restricting the analysis to the upper half plane. The material parameters adopted were $v_0 = 0.25$, $\sigma_0/E_0 = 9.1 \times 10^{-4}$ and $\sigma_s/\sigma_0 = 1.2$; see Fig. 1b. The applied loads were increased proportionally and monotonically up to a value resulting in damage over roughly one-third of the mesh. The discretized field equations were integrated by means of a forward-Euler scheme.

Figure 8 shows a comparison of mode I angular stress fields at the point of maximum load. Shown are the exact analytical solution, which in this case coincides with the linear elastic fields, and the results of the finite element computations on the second ring of elements. The comparison thus exhibits the level of accuracy of the computed stresses.

Figure 9 shows the saturated and damaged zones at maximum load for various mixities. For mode I, Fig. 9a, the expected symmetric configurations are obtained. The sizes r_s and r_d of both zones, measured along the plane of the crack, correlate quite closely with the estimates

$$r_s = \frac{1}{2\pi}\left(\frac{K_I^{tip}}{\sigma_s}\right)^2, \quad r_d = \frac{1}{2\pi}\left(\frac{K_I^{tip}}{\sigma_0}\right)^2. \tag{14}$$

As the mode II component is increased, the saturated and damage zones experience an
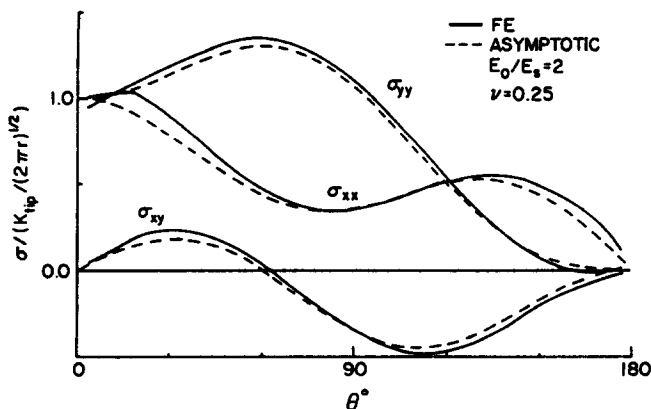

Fig. 8. Comparison of computed and exact asymptotic stress fields.

overall rotation; Figs 9b–9d. As noted in connection with the asymptotic solutions, this leaves a sector of material $(\pi - \theta^e) \leqslant \theta \leqslant \pi$ unshielded, the size of which increases with the extent of mode II in the remote loads. For mode I, the radius $r_d(\theta)$ of the damaged zone steadily increases as θ goes from $\pi - \theta^e$, where σ_1 and r_d vanish, to $-\pi$, where σ_1 and r_d attain their maximum values.

Figure 10 shows the relation between the mixities of the remote and near-tip stress fields. Remarkably, one has

$$M^d \approx M^e \qquad\qquad (15)$$

to within the accuracy of the analysis. Figure 11, on the other hand, depicts the value of the J integral of Rice computed from circular contours of varying radii. The results were obtained using the domain-J method of Shih *et al.* (1986). It is seen that, for the family of integration contours under consideration, the J integral is ostensibly path independent.

Under these conditions, it is possible to determine the relation between the remote and near-tip stress intensity factors from the sole knowledge of the asymptotic singular fields. By computing J based on a contour far into the elastic zone, one obtains the familiar result
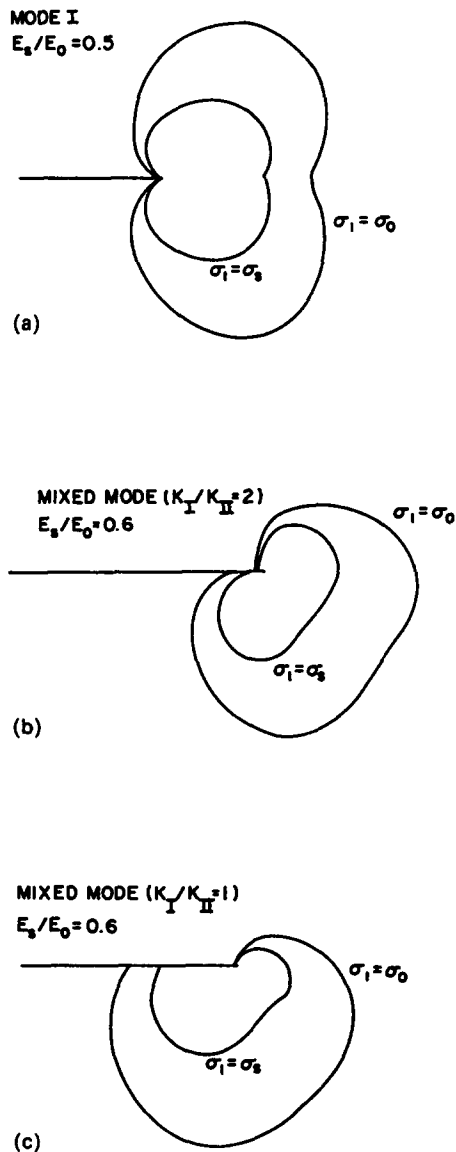
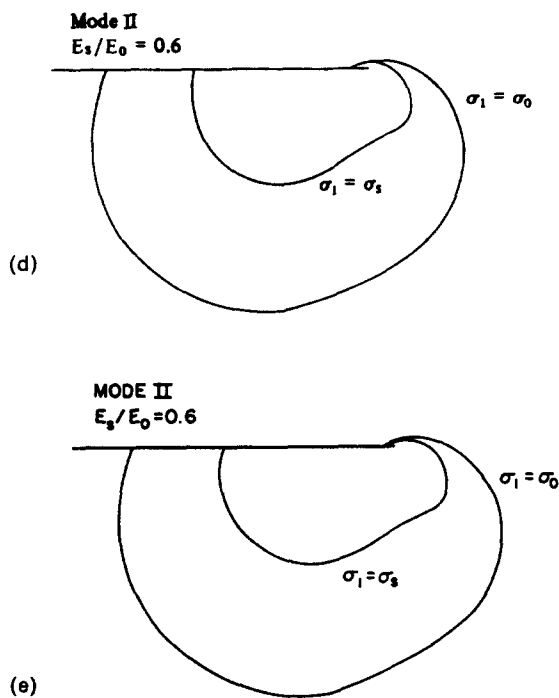Fig. 9. Saturated and damaged regions.

Mode II
$E_s/E_0 = 0.6$

$\sigma_1 = \sigma_0$

$\sigma_1 = \sigma_s$

(d)

MODE II
$E_s/E_0 = 0.6$

$\sigma_1 = \sigma_0$

$\sigma_1 = \sigma_s$

(e)

Fig. 9—Continued.

$$J_\infty = \frac{1-v_0^2}{E_0}[(K_I^\infty)^2 + (K_{II}^\infty)^2].$$ (16)

Using a contour shrunk to the crack tip one obtains

$$J_{tip} = \frac{1-v_0^2}{E_0}[(K_I^{tip})^2 + (K_{II}^{tip})^2] + \lambda_s f(K_I^{tip}, K_{II}^{tip})$$ (17)

where f is a homogeneous function of degree two which can be determined directly from the asymptotic solution. By the path independence of J, one has
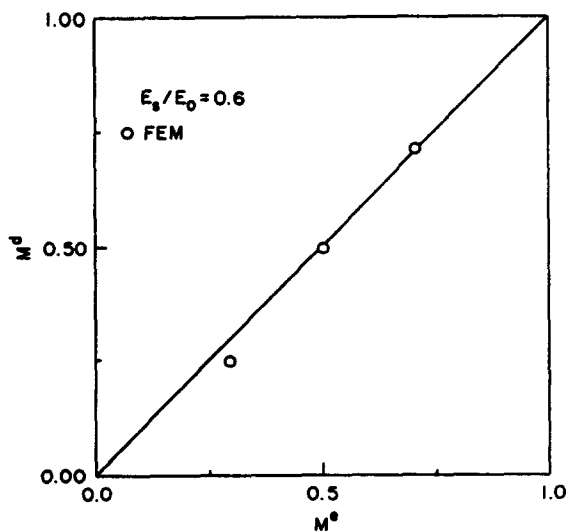
$E_s/E_0 = 0.6$
O FEM

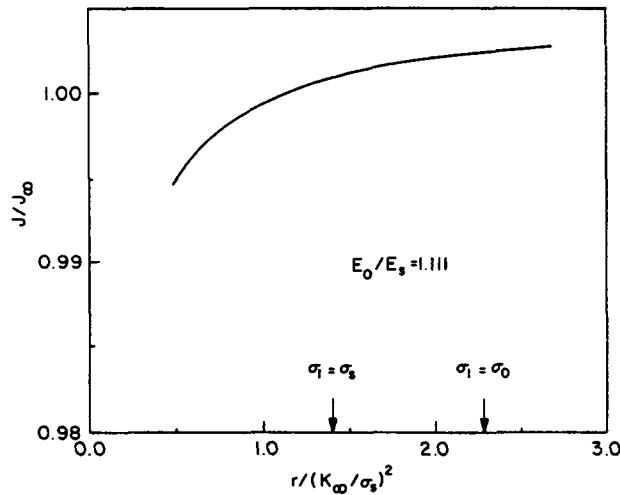Fig. 10. Relation between mixities of near-tip and remote stress fields.

Fig. 11. Variation of J integral computed along concentric circular paths.

$$J_{\text{tip}} = J_\infty. \tag{18}$$

On the other hand, (15) implies the relation

$$\frac{K_{\text{I}}^{\text{tip}}}{K_{\text{II}}^{\text{tip}}} = \frac{K_{\text{I}}^\infty}{K_{\text{II}}^\infty}. \tag{19}$$

Equations (18) and (19), together with (16) and (17), suffice to uniquely determine $K_{\text{I}}^{\text{tip}}$ and $K_{\text{II}}^{\text{tip}}$ as a function of K_{I}^∞ and K_{II}^∞. For instance, for pure mode II loading, eqns (18) and (19) reduce to the single relation

$$\frac{1 - v_0^2}{E_0}(K_{\text{II}}^\infty)^2 = \left[\frac{1 - v_0^2}{E_0} + \beta\lambda_s\right](K_{\text{II}}^{\text{tip}})^2 \tag{20}$$

where, from the asymptotic solution, the coefficient β is numerically determined to take the value 0.82. From (20) one obtains the dependence of the mode II shielding ratio $K_{\text{II}}^{\text{tip}}/K_{\text{II}}^\infty$ on E_0/E_s depicted in Fig. 6.

A question closely related to the path invariance of J concerns the near-proportionality of the stress paths at material points within the body. Near-proportionality was also an underlying assumption throughout the asymptotic analysis of Section 2, which was based on a deformation theory of damage. The question thus arises of how closely these conditions are realized in the field solution. Shown in Fig. 12a are the stress paths undergone by a quadrature point adjacent to the crack plane on the second ring of elements. The results correspond to pure mode I loading. As may be seen, the paths remain ostensibly proportional to within the accuracy of the analysis. A similar situation is encountered in the mixed mode and mode II cases. Figure 12b depicts the stress paths computed at an angle $\theta = 120°$ to the plane of the crack for pure mode II. As in the case of mode I loading, conditions of near-proportionality are closely realized. These observations lend a posteriori justification to the use of a deformation theory of damage and to the presumption of path independence of the J integral.

A final issue of critical importance concerns the range of dominance of the computed asymptotic fields. For an asymptotic solution to be of relevance to the fracture behavior of a solid, it must dominate over a distance to the crack tip well in excess of the region where the actual micromechanical processes of separation take place (see, e.g., Hutchinson, 1983, for a detailed discussion). This requirement is not always satisfied. In fact, asymptotic solutions are known which possess a vanishing region of dominance. Under conditions of
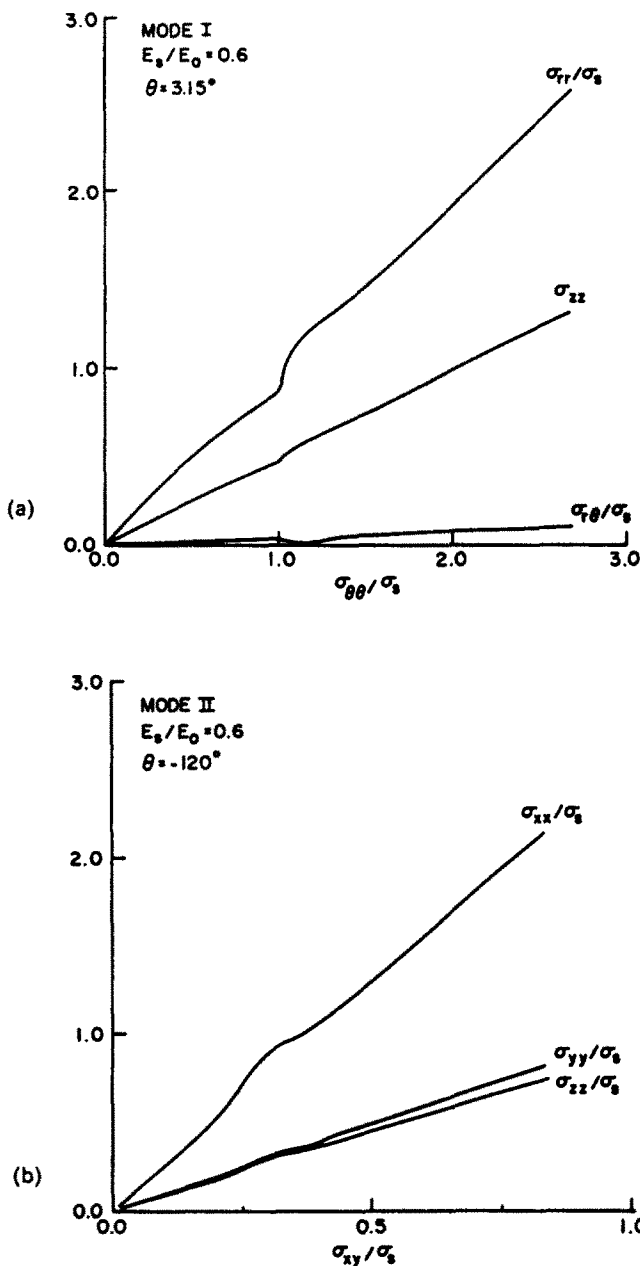
Fig. 12. Stress paths at selected points in the vicinity of the crack tip.

dominance, however, the process zone is driven by the surrounding singular fields, and the critical conditions for crack growth are expressible in terms of K_I^{tip} and K_{II}^{tip}.

The question of dominance is assessed here by a direct comparison of the finite element and asymptotic solutions. Figure 13 shows the ratio of the full field to the asymptotic $\sigma_{\theta\theta}$ field on a radius adjacent to the plane of the crack. The results correspond to pure mode I loading and are shown for remote loads which result in a damage zone extending to roughly one-third of the total mesh. As may be seen, the singular field dominates out to a distance ahead of the tip of

$$r_d/5 \leqslant R \leqslant r_d/4. \tag{21}$$

This situation parallels that encountered in metals. Similar observations apply to the mixed mode case.
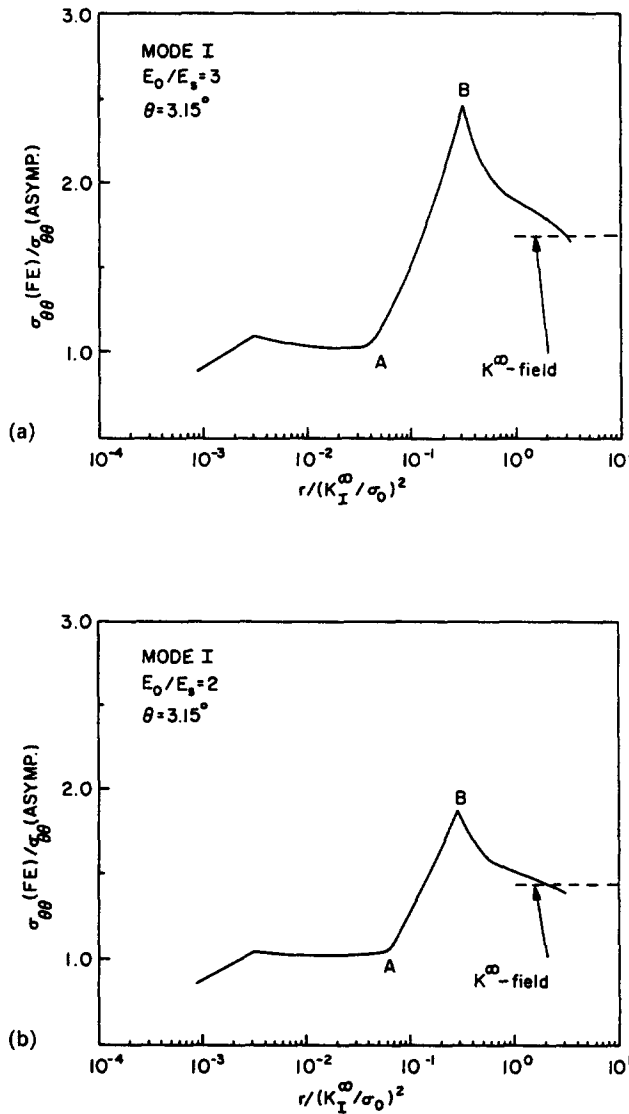
Fig. 13. Comparison between asymptotic and full field solutions.

In monolithic ceramics, macrocracks grow primarily by coalescence with the micro-cracks in the immediate vicinity of the crack tip. Thus, the size of the process zone is determined by the distance between the tip and the leading microcrack, and, hence, by the spacing l between the microcracks. An analysis of Ortiz (1988) based on a cohesive zone model lends additional support to this scenario. Thus, the condition for dominance becomes

$$R \gg l. \tag{22}$$

Inserting estimates (21) and (22) into this condition, one obtains restrictions on the geometry of the cracked body and on the magnitude of the applied loads. Compliance with these restrictions insures dominance of the singular fields. It is noteworthy that (22) is also a requirement for the analysis given here to apply, namely, that the zone of damage be large compared to the mean spacing of the microcracks. Both the conditions for dominance and the applicability of the method of analysis may break down, for instance, for short cracks. In this case, the surrounding microcracks cannot be idealized as a homogeneized continuum, and the discrete nature of the interactions needs to be taken into account. In particular, the singular fields computed with the aid of models of distributed damage become physically meaningless.

Short cracks arise in ceramics during the first stages of microcrack coalescence, the mechanism responsible for the ultimate failure of the material. Following the inception of coalescence, the short-range interactions between a small number of critical microcracks become all-important and models of distributed damage no longer apply. On the other hand, as discussed above, the small-scale damage concepts of fracture mechanics are equally inapplicable until the critical flaw becomes sufficiently large to possess dominant near-tip singular fields. Thus, incipient microcrack coalescence arises as a purely micromechanical phenomenon not amenable to treatment within the confines of either classical constitutive theory or small-scale damage fracture mechanics.

Under conditions of dominance, the conditions at the crack tip are fully determined by the asymptotic singular fields, which may be thought of as driving the growth of the crack. Thus, for instance, crack growth may then be reasonably assumed to occur when K_I^{tip}, in mode I, or a suitable combination of K_I^{tip} and K_{II}^{tip}, under mixed mode conditions, attain a critical value characteristic of the toughness of the material. It bears emphasis that the validity of postulates of this type is critically dependent on the dominance of the asymptotic fields used to characterize the conditions prevailing at the crack tip, and hence the need for establishing such dominance.

5. SUMMARY AND CONCLUSIONS

Asymptotic and full field solutions have been obtained for a semi-infinite crack in a monolithic ceramic under mixed mode I–mode II loading. Mixed loading had not heretofore been considered in the literature on the subject, which has been primarily concerned with the mode I case. The mixed mode asymptotic fields have been herein computed by means of a new finite element method described in the Appendix. The principal advantage of the present approach over traditional finite differences or shooting methods is that the constitutive relations enter the formulation undifferentiated. In this fashion, the numerical calculations are greatly simplified. The method has exhibited remarkably good accuracy for relatively coarse meshes.

A salient feature of the mixed asymptotic solutions obtained here which does not arise under mode I loading is the presence of an elastic wedge of material free of microcracking. A consequence of this elastic wedge is that the crack tip is less shielded by damage under mixed mode conditions than in pure mode I. This effect is also revealed by the computed shielding ratios, or ratio between the remotely applied and near-tip stress intensity factors. Thus, the shielding ratio in mode I is about 10% lower than that which is computed for mode II. These observations are in keeping with the available experimental data (Shetty et al., 1981; Morrone and Suresh, 1988). As in the mode I case (Ortiz, 1987), the singular strain fields exhibit discontinuities. The character and magnitude of the jumps have been determined analytically.

A number of assumptions pervade past work on the subject which require careful justification. For instance, the relation between near-tip and remote stress intensity factors has been frequently determined using the invariance of the J integral (see, e.g., Charalambides and McMeeking, 1987; Hutchinson, 1987; Ortiz, 1987). This, however, presumes that the constitutive response at all points within the solid is indistinguishable from that of a nonlinear elastic material. This assumption is justified only if the stress paths remain nearly proportional at all times. To elucidate this issue, a full field solution, rather than an asymptotic solution, is needed. We have computed full field solutions using conventional finite elements for mixities ranging from mode I to mode II conditions. Our results show that, for the full range of mixities, proportional stressing is indeed closely realized.

Another feature of the solution which is revealed by the full field analysis is the fact that the mixity of the near-tip singular fields ostensibly coincides with the mixity of the remotely applied K-fields. This result, in conjunction with the invariance of the J integral, suffices to relate the magnitude of the remote and near-tip stress intensity factors over the full range of mixities.

Finally, we have addressed the issue of dominance of the asymptotic singular fields. In essence, asymptotic solutions are useful in characterizing crack growth only if they

dominate over distances much larger than the size of the process zone. This is the region close to the crack tip where the processes of separation resulting in the growth of the crack, in this case coalescence with the neighboring microcracks, take place. For the materials considered here, the size of the process zone is a small multiple of the distance between microcracks (Ortiz, 1987), which is itself commensurate with the grain size. The range of dominance of an asymptotic field may be assessed by comparison to the full field solution. For the mode I case, we have determined that the singular fields obtained here dominate out to distances ahead of the tip of the order of 1/5–1/4 of the damaged region. These bounds are of the same order as those pertaining to the HRR singularity of small scale yielding fracture mechanics (see, e.g., Hutchinson, 1983).

The dominance requirement sets restrictions on the geometry of the body and on the magnitude of the loads for crack growth to be driven by the asymptotic singular fields. In particular, when these restrictions are met, the critical conditions for crack growth are expressible in terms of the near-tip stress intensity factors. It should be emphasized that dominance is not an assured property of all asymptotic fields. In fact, asymptotic solutions have been obtained in fracture mechanics which have been shown to possess a vanishing range of dominance. In the case of ceramic materials, our results indicate that lack of dominance is a characteristic of short cracks. The analysis of short cracks is central to the understanding of the early stages of coalescence. In this case, the discrete interactions between the crack and the surrounding microcracks play an important role, and models of distributed damage are no longer appropriate.

REFERENCES

Amazigo, J. C. and Hutchinson, J. W. (1977). Crack-tip fields in steady crack growth with linear strain hardening. *J. Mech. Phys. Solids* **25**, 81–97.

Budiansky, B., Hutchinson, J. W. and Lambropoulos, J. C. (1983). Continuum theory of dilatant tansformation toughening in ceramics. *Int. J. Solids Structures* **19**, 337–355.

Charalambides, P. G. (1986). Near tip mechanics of stress induced microcracking in brittle materials. Ph.D. Thesis, University of Illinois, Urbana–Champaign.

Charalambides, P. G. and McMeeking, R. M. (1987). Finite element method simulation of crack propagation in a brittle microcracking solid. *Mech. Mater.* **6**, 71–87.

Claussen, N. (1976). Fracture toughness of Al_2O_3 with an unstabilized ZrO_2 dispersed phase. *J. Am. Ceram. Soc.* **59**, 49–51.

Evans, A. G. (1984). Aspects of the reliability of ceramics. In *Defect Properties and Processing of High-technology Nonmetallic Materials* (Edited by J. H. Crawford, Y. Chen and W. A. Sibley), pp. 63–80. North-Holland, Amsterdam.

Evans, A. G. and Fu, Y. (1985). Some effects of microcracks on the mechanical properties of brittle solids—II. Microcrack toughening. *Acta Metall.* **33**, 1525–1531.

Faber, K. T. and Evans, A. G. (1983a). Crack deflection processes—I. Theory. *Acta Metall.* **31**, 565–576.

Faber, K. T. and Evans, A. G. (1983b). Crack deflection processes—II. Experiment. *Acta Metall.* **31**, 577–584.

Fu, Y. (1983) Mechanics of microcrack toughening in ceramics. Ph.D. Thesis, University of California, Berkeley.

Gong, S. and Horii, H. (1987). General solution to the problem of microcracks near the tip of a main crack. Report 87-12, Department of Civil Engineering, University of Tokyo, December 1987.

Gurtin, M. E. (1984). The linear theory of elasticity. In *Mechanics of Solids*, Vol. II, pp. 1–295.

Hayhurst, D. R. (1972). Creep rupture under multi-axial states of stress. *J. Mech. Phys. Solids* **20**, 381–390.

Hayhurst, D. R. and Leckie, F. A. (1973). The effect of creep constitutive and damage relationships upon the rupture time of a solid circular torsion bar. *J. Mech. Phys. Solids* **21**, 431–446.

Hoagland, R. G. and Embury, J. D. (1980). A treatment of inelastic deformation around a crack tip due to microcracking. *J. Am. Ceram. Soc.* **63**, 404–410.

Hoagland, R. G., Hahn, G. T. and Rosenfield, A. R. (1973). Influence of microstructure on the fracture propagation in rock. *Roc. Mech.* **5**, 77–106.

Hutchinson, J. W. (1983). Fundamentals of the phenomenological theory of nonlinear fracture mechanics. *J. Appl. Mech.* **50**, 1042–1051.

Hutchinson, J. W. (1987). Crack tip shielding by micro-cracking in brittle solids. *Acta Metall.* **35**(7), 1605–1619.

Kachanov, M. (1986). On crack–microcrack interactions. *Int. J. Fracture* **30**, 65–72.

Kranz, R. L. (1983). Microcracks in rocks, a review. *Tectonophysics* **100**, 449.

Morrone, A. and Suresh, S. (1988). Mixed mode fracture of ceramic materials: combined mode I–mode II and mode I–mode III. Submitted for publication.

Ortiz, M. (1985). A constitutive theory for the inelastic behavior of concrete. *Mech. Mater.* **4**, 67–93.

Ortiz, M. (1987). A continuum theory of crack shielding in ceramics. *J. Appl. Mech.* **54**, 54–58.

Ortiz, M. (1988). Microcrack coalescence and macroscopic crack growth initiation in brittle solids. *Int. J. Solids Structures* **24**, 231–250.

Ortiz, M. and Giannakopoulos, A. E. (1989). Maximal crack-tip shielding by microcracking. *J. Appl. Mech.* **16**, 279–283.
Ortiz, M. and Molinari, A. (1988). Microstructural thermal stresses in ceramic materials. *J. Mech. Phys. Solids* **36**, 385–400.
Rice, J. R. (1968). Mathematical analysis in the mechanics of fracture. In *Fracture* (edited by H. Liebowitz), Vol. 2, pp. 191–311. Academic Press, New York.
Rodin, G. (1987). An example of crack tip analysis in brittle damaged materials. *Int. J. Fracture* **33**, 31–35.
Shetty, D. C. and Rosenfield, A. R. and Duckworth, W. H. (1981). Mixed mode fracture of ceramics in diametral compression. *J. Am. Ceram. Soc.* **69**, 437–443.
Shih, C. F. (1973). Elastic–plastic analysis of combined mode crack problems. Ph.D. Thesis, Harvard University.
Shih, C. F., Moran, B. and Nakamura, T. (1986). Energy release rate along a three-dimensional crack front in thermally stressed body. *Int. J. Fracture* **30**, 79–102.
Suresh, S. and Brockenbrough, J. (1988). A theory for creep by interfacial flaw growth in ceramics and ceramic composites. *Acta Metall.*, **36**, 1455–1470.
Swanson, P. L., Fairbanks, C. J., Lawn, B. R., Mai, Y. W. and Hockey, B. J. (1987). Crack-interface grain bridging as a fracture-resistance mechanism in ceramics—I. Experimental study in alumina. *J. Am. Ceram. Soc.* **70**, 279–289.
Symington, M., Ortiz, M. and Shih, C. F. (1989). A finite element method for the computation of asymptotic crack tip fields. *Int. J. Fracture* (in press).
Wu, C. C., Freiman, S. W., Rice, R. W. and Mecholsky, J. J. (1978). Microstructural aspects of crack propagation in ceramics. *J. Mater. Sci.* **13**, 2659–2670.
Zienkiewicz, O. C. (1977). *The Finite Element Method*, 3rd Edn. McGraw-Hill, Scarborough, CA.

APPENDIX: A FINITE ELEMENT METHOD OF ASYMPTOTIC ANALYSIS

The angular components of asymptotic singular fields in fracture mechanics have been traditionally computed by means of finite difference (Amazigo and Hutchinson, 1977) or shooting methods (Shih, 1973). Both techniques deal directly with the governing fourth-order ODE. Since the formulation of the governing equation requires differentiating the constitutive relations twice, the analysis may become exceedingly cumbersome for complex material models. The finite element method, by contrast, is based on a weak integral statement of the governing ODE, wherein the constitutive relations enter undifferentiated. By virtue of this restatement of the problem, the numerical calculations are greatly simplified. In this Appendix, the finite element method adopted in the computation of the asymptotic fields presented in Section 3 is described in summary form. A more detailed exposition of the method may be found in the article of Symington *et al.* (1989).

The point of departure for the method is the equation of compatibility

$$\tilde{\varepsilon}_{rr}'' + \alpha\tilde{\varepsilon}_{rr} - \alpha(1-\alpha)\tilde{\varepsilon}_{\theta\theta} - (1-\alpha)\tilde{\gamma}_{r\theta}' = 0 \tag{A1}$$

for separable strain fields of the form

$$\varepsilon_{\alpha\beta} \propto r^{-\alpha}\tilde{\varepsilon}_{\alpha\beta}(\theta). \tag{A2}$$

Equation (A1) is obtained simply by inserting (A2) into the two-dimensional equation of compatibility in polar coordinates.

The method diverges from shooting and finite difference schemes in that (A1) is recast in weak form, in the spirit of finite elements. To obtain the weak form of (A1), multiply through by an arbitrary weighting function η satisfying the homogeneous essential boundary conditions

$$\eta(-\pi) = \eta(\pi) = 0, \quad \eta'(-\pi) = \eta'(\pi) = 0, \tag{A3}$$

integrate over the range $[-\pi, \pi]$ and integrate by parts twice, to arrive at the integral statement

$$\int_{-\pi}^{\pi} [(\eta'' + \alpha\eta)\tilde{\varepsilon}_{rr} - \alpha(1-\alpha)\eta\tilde{\varepsilon}_{\theta\theta} + (1-\alpha)\eta'\tilde{\gamma}_{r\theta}] \, d\theta = 0. \tag{A4}$$

This equation may be rephrased in a more compact form by introducing the following strain vector $\tilde{\varepsilon}$ and operator $\mathbf{L}$

$$\tilde{\varepsilon} \equiv \begin{Bmatrix} \tilde{\varepsilon}_{rr} \\ \tilde{\varepsilon}_{\theta\theta} \\ \tilde{\gamma}_{r\theta} \end{Bmatrix}, \quad \mathbf{L}\eta \equiv \begin{Bmatrix} \eta'' + \alpha\eta \\ -\alpha(1-\alpha)\eta \\ (1-\alpha)\eta' \end{Bmatrix} \tag{A5}$$

whereupon (A4) becomes

$$\int_{-\pi}^{\pi} (\mathbf{L}\eta)^{\mathrm{T}}\tilde{\varepsilon} \, d\theta = 0. \tag{A6}$$

Next, assume that the stress potential ϕ is separable, i.e. it is of the form

$$\phi \propto r^{2-\beta} f(\theta). \tag{A7}$$

Then the stresses are themselves separable and may be written as

$$\sigma_{\alpha\beta} \propto r^{-\beta} \tilde{\sigma}_{\alpha\beta}(\theta), \tag{A8}$$

where the angular distributions are given by

$$\tilde{\sigma} \equiv \begin{Bmatrix} \tilde{\sigma}_{rr} \\ \tilde{\sigma}_{\theta\theta} \\ \tilde{\sigma}_{r\theta} \end{Bmatrix} = \begin{Bmatrix} f'' + (2-\beta)f \\ (2-\beta)(1-\beta)f \\ -(1-\beta)f' \end{Bmatrix} \equiv \mathbf{R}f. \tag{A9}$$

Finally, assume that the constitutive equations are homogeneous of some degree. Then, a relation of the type

$$\tilde{\varepsilon} = \tilde{\varepsilon}(\tilde{\sigma}) \tag{A10}$$

between the angular components of stress and strain follows. Inserting (A9) and (A10) into (A6), one finds

$$\int_{-\pi}^{\pi} (\mathbf{L}\eta)^{\mathsf{T}} \tilde{\varepsilon}(\mathbf{R}f) \, d\theta = 0. \tag{A11}$$

This integral statement may now be taken as a basis for formulating finite element approximations. To this end, the domain $[-\pi, \pi]$ is partitioned into a collection of two-noded elements. Since the weak form (A6) involves derivatives of second order in the unknown function, piecewise continuously differentiable interpolation must be used to obtain convergent approximations. In one-dimensional problems such as the one under consideration here, this may be accomplished simply through the use of Hermitian interpolation. The unknowns of the problem thus become the nodal values of the stress potential f_a and its derivatives f'_a, where a ranges over all nodes in the finite element mesh. Using standard techniques (see, e.g., Zienkiewicz, 1977) the discretized problem may be reduced to the solution of a homogeneous system of nonlinear equations

$$\mathbf{F}(\mathbf{u}) = \mathbf{0} \tag{A12}$$

where $\mathbf{u}$ signifies the array of nodal degrees of freedom $\{f_a, f'_a\}$. This may be solved with the aid of standard nonlinear solution procedures such as Newton–Raphson's method.

The collection of all solutions of (A12) may be parametrized by means of the amplitude of the potential $f(\theta)$ at some node and the location of its point of zero crossing. These subsidiary constraints may be enforced as additional boundary conditions. By moving the location of the zero of f one obtains solutions of varying mixities. For instance, pure mode II is obtained by taking the zero crossing to be at $\theta = 0$, whereas pure mode I follows from the choice $\theta = \pi$.